

Enhancing angular sampling rate of integral floating display using dynamically variable apertures

Jisoo Hong, Jiwoon Yeom, and ByoungHo Lee*

School of Electrical Engineering, Seoul National University, Gwanak-Gu Gwanakro 1, Seoul 151-744, South Korea
*byoungHo@snu.ac.kr

Abstract: Two novel methods are proposed which enhance the angular sampling rate of the integral floating display by adopting dynamically variable apertures in front of the lenslet array or the floating lens. Adopted dynamically variable apertures are opened sequentially in synchronization with proper elemental images to subdivide the angular sampling step by time-multiplexing method. Our proposed method can enhance the angular sampling rate, which is related to an expressible longitudinal range, without sacrificing other visual quality factors in tradeoff relationship. Especially, our proposed method with apertures on the floating lens provides two-dimensional/three-dimensional convertible feature to integral floating display system.

©2012 Optical Society of America

OCIS codes: (110.2990) Image formation theory; (100.6890) Three-dimensional image processing.

References and links

1. J. Hong, Y. Kim, H.-J. Choi, J. Hahn, J.-H. Park, H. Kim, S.-W. Min, N. Chen, and B. Lee, "Three-dimensional display technologies of recent interest: principles, status, and issues [Invited]," *Appl. Opt.* **50**(34), H87–H115 (2011).
 2. P. Benzie, J. Watson, P. Surman, I. Rakkolainen, K. Hopf, H. Urey, V. Sainov, and C. von Kopylow, "A survey of 3DTV displays: techniques and technologies," *IEEE Trans. Circ. Syst. Video Tech.* **17**(11), 1647–1658 (2007).
 3. B. Javidi and F. Okano, eds., *Three Dimensional Television, Video, and Display Technology* (Springer, 2002).
 4. S.-W. Min, M. Hahn, J. Kim, and B. Lee, "Three-dimensional electro-floating display system using an integral imaging method," *Opt. Express* **13**(12), 4358–4369 (2005).
 5. J. Kim, S.-W. Min, and B. Lee, "Viewing region maximization of an integral floating display through location adjustment of viewing window," *Opt. Express* **15**(20), 13023–13034 (2007).
 6. J. Kim, S.-W. Min, Y. Kim, and B. Lee, "Analysis on viewing characteristics of an integral floating system," *Appl. Opt.* **47**(19), D80–D86 (2008).
 7. J. Kim, S.-W. Min, and B. Lee, "Floated image mapping for integral floating display," *Opt. Express* **16**(12), 8549–8556 (2008).
 8. J. Kim, G. Park, Y. Kim, S.-W. Min, and B. Lee, "Elimination of image discontinuity in integral floating display by using adaptive image mapping," *Appl. Opt.* **48**(34), H176–H185 (2009).
 9. J.-H. Park, K. Hong, and B. Lee, "Recent progress in three-dimensional information processing based on integral imaging," *Appl. Opt.* **48**(34), H77–H94 (2009).
 10. F. Okano, J. Arai, and M. Kawakita, "Wave optical analysis of integral method for three-dimensional images," *Opt. Lett.* **32**(4), 364–366 (2007).
 11. D.-H. Shin, B. Lee, and E.-S. Kim, "Multidirectional curved integral imaging with large depth by additional use of a large-aperture lens," *Appl. Opt.* **45**(28), 7375–7381 (2006).
 12. R. Martínez-Cuenca, H. Navarro, G. Saavedra, B. Javidi, and M. Martínez-Corral, "Enhanced viewing-angle integral imaging by multiple-axis telecentric relay system," *Opt. Express* **15**(24), 16255–16260 (2007).
 13. S.-W. Min, J. Kim, and B. Lee, "New characteristic equation of three-dimensional integral imaging system and its applications," *Jpn. J. Appl. Phys.* **44**(2), L71–L74 (2005).
 14. F. Jin, J. S. Jang, and B. Javidi, "Effects of device resolution on three-dimensional integral imaging," *Opt. Lett.* **29**(12), 1345–1347 (2004).
 15. Y. Takaki, Y. Urano, S. Kashiwada, H. Ando, and K. Nakamura, "Super multi-view windshield display for long-distance image information presentation," *Opt. Express* **19**(2), 704–716 (2011).
-

1. Introduction

Three-dimensional (3D) display has a long history of about 170 years since the first invention of Wheatstone's stereoscope [1]. It has passed just a few years since the first successful commercial 3D display was released in the mass market. Some major manufacturers have started to supply the 3D displays based on the stereoscopy, which requires the users to wear a special apparatus. Because of inconvenience of stereoscopy, the next step of commercialization will apparently be the autostereoscopic display. There are a number of candidates for the autostereoscopic display ranging from the multi-view display such as parallax barrier, to the volumetric display such as holography [2, 3]. It is hard to predict which one will be the first mass commercial autostereoscopic product because each has pros and cons. Yet, considering the present status of the display device, further developments are needed for the existing autostereoscopic display methods.

Integral floating display is a 3D display method that combines integral imaging (InIm) and floating technology using a convex lens [4–8]. By adopting an additional convex lens, integral floating touts advantageous features than InIm in various aspects. InIm, which was first proposed by Lippmann in 1908, provides autostereoscopic 3D images with continuous viewpoints [9]. However, InIm usually suffers from bottlenecks related to viewing angle and expressible depth range [10–12]. Integral floating display is known to provide larger viewing angle and depth expression than InIm itself. And the borderlines of lenslet array, which are one factor that deteriorates visual quality of InIm scheme, are also eliminated from displayed 3D images. However, the enhanced performance by adopting additional convex lens raises drawback in other aspect. Three visual quality factors of displayed 3D images by InIm scheme is restricted by the relationship

$$R_l^2 \Delta z_m \tan\left(\frac{\Omega}{2}\right) = \frac{1}{p}, \quad (1)$$

where R_l is the resolution of the integrated image, Δz_m is the expressible longitudinal range, Ω is the viewing angle of InIm, and p is the pixel pitch of the display device [13]. It demonstrates that the pixel pitch of display device is a fundamental resource that rules the visual quality of InIm system. Hence, without a reduction in size of pixels, some feature might be enhanced by diminishing other features. Although Eq. (1) was developed by considering InIm, the main idea of this tradeoff relationship – the pixel pitch of display is a fundamental resource that rules characteristic of 3D display – is generally applicable to integral floating display as well. The cost for the advantages of integral floating display listed above is low angular sampling rate. It is a cause of discontinuity in motion parallax which makes the integral floating system be ranked at the level of multi-view display, which allows the observer to be positioned only at some discrete points. In the previous research conducted by our group, it has been proposed to deal with this problem with tracking method which requires the observer to wear a special apparatus [8]. This approach, though it is definitely one viable solution, has problems in that it is out of sense of autostereoscopy and there is a limitation in the number of observers.

In this paper, we propose two methods that enhance the angular sampling rate of integral floating display by using dynamically variable apertures. Our newly proposed method approaches the issue in the direction of increasing the fundamental resource for visual quality with the aid of time-multiplexing. In the following sections, we will describe the principle of the proposed scheme. And the experimental results will be provided to verify our method.

2. Effect of angular sampling rate in integral floating system

Integral floating also has a tradeoff relationship among visual quality factors for the given specifications of the system. The relationship among the size of viewing window, the resolution of floated image and the expressible longitudinal range had been investigated in [6]. The expressible longitudinal range was analyzed in the viewpoint of the wave optics.

However, for the usually considered specifications, it is rather ruled by the ray optics. In this section, we will analyze the expressible longitudinal range of integral floating display in the ray optic viewpoint and investigate its relation with the angular sampling rate.

One way to assess the performance of 3D display is to investigate the available voxels provided by the system. Jin *et al.* has revealed that the voxels of InIm system are available at farthest Ng from the lenslet array, where N is the number of pixels per lenslet and g is the distance between the elemental image and the lenslet array [14]. The available voxels of integral floating can be investigated in a similar way.

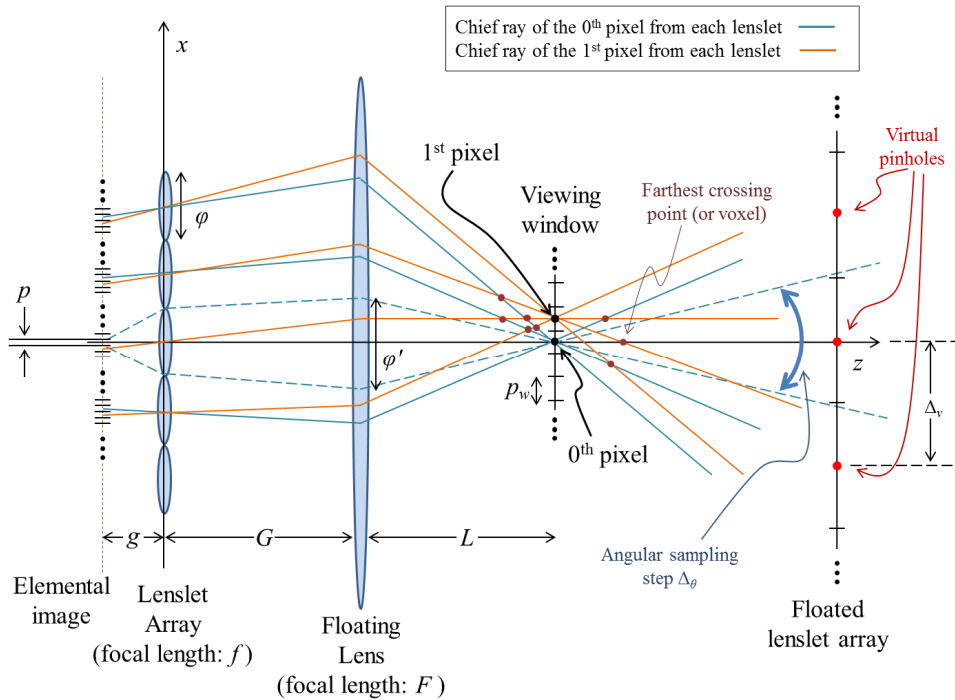


Fig. 1. Display principle of integral floating system. Some crossing points of chief rays, which are considered as available voxels, are illustrated as dots for reference.

Figure 1 shows a diagram that describes the display principle of integral floating scheme where a lenslet array with focal length f and a floating lens with focal length F have been adopted. The gap between the elemental image, whose pixel pitch is p , and the lenslet array is indicated as g . Though the figure illustrates the case of $g < f$, the analysis given here is applicable for other cases. And G represents the gap between the lenslet array and the floating lens. On the left-side of the floating lens, the elemental image is imaged by the lenslet array and its image creates a so-called central depth plane by the principle of InIm. On the right side of the floating lens, the viewing window is formed by a floated image of the central depth plane and it can be interpreted as an imaginary display screen. Chief rays from each lenslet pass through the viewing window covering all pixels on the viewing window. And they are collected at the center of corresponding lenslet of the floated lenslet array. Hence, the center of each floated lenslet can be considered as a pinhole of the virtual pinhole camera in calculating the elemental image. Chief rays from different lenslet provide directional rays for each pixel on the viewing window. The way that the viewing window, which is L distant from the floating lens, provides 3D information is very close to InIm scheme. Following the method suggested in [14], the farthest available voxel can be determined by finding the crossing point of chief rays from center and adjacent pixels, which are labeled as the 0th and 1st pixels, respectively, on viewing window. The expressible longitudinal range, which is

estimated considering available voxels, in front and behind of the viewing window is easily calculated as

$$\Delta_z = \frac{(F/(G-F))^2 \varphi^2 |L| p_w / \varphi'}{(h_u - p_w)(p_w - h_l)}, \quad (2)$$

where h_u and h_l are the lateral positions of virtual pinholes just above and below the 1st pixel on the viewing window, respectively. p_w is the pixel pitch of the viewing window and φ' is the lateral range on the floating lens covered by the rays from one point light source on the elemental image. The average value of each term in the denominator of Eq. (2) is the half of the interval between virtual pinholes given by

$$\Delta_v = \varphi \frac{F}{G-F}. \quad (3)$$

Equation (2) can be represented by the average case as

$$\Delta_{z,avg} = 4 \frac{L}{\varphi'} p_w. \quad (4)$$

Though the angular sampling step varies with the location of pixel on viewing window, the angular sampling rate of the integral floating system can be represented by the sampling step of center ray of center pixel on the viewing window, which is indicated as Δ_θ in Fig. 1. By using Δ_θ , we define the angular sampling rate of the integral floating system as

$$R_\theta = \frac{1}{\Delta_\theta} \approx \frac{L}{\varphi'}, \quad (5)$$

where the approximation holds when Δ_θ is sufficiently small. Hence, the expressible longitudinal range of integral floating system depends on the angular sampling rate at the viewing window when we consider the voxels created by the integral floating system.

The performance of integral floating display can also be assessed in the aspect of visual quality perceived by the observer. The motion parallax is one of the important physiological cues which provide 3D information to the observer. However, integral floating display is known to have discontinuity in the motion parallax because the displayed image does not change inside consecutive viewing zones whose lateral sizes are determined by Eq. (3) [8]. Such discontinuity causes bother to the observer. Hence the lateral size of the viewing zone, which is related to the angular sampling rate, should be excessively reduced until the discontinuity is not perceived by the observer to guarantee the continuous viewpoints unlike multi-view displays. Takaki *et al.* has argued that it can be satisfied under the condition where the discontinuity in motion parallax can be neglected considering the angular resolution of display device [15]. Similar investigation can be applied for the integral floating display.

As shown in Fig. 2, because of the discontinuity in motion parallax, there exists uncertainty in the lateral position of a target voxel, which is out of the longitudinal position of the viewing window. The condition for neglecting the discontinuity in motion parallax is that this uncertainty should be smaller than the pixel pitch of the viewing window in angular sense. Referring to Fig. 2, the condition can be easily calculated as

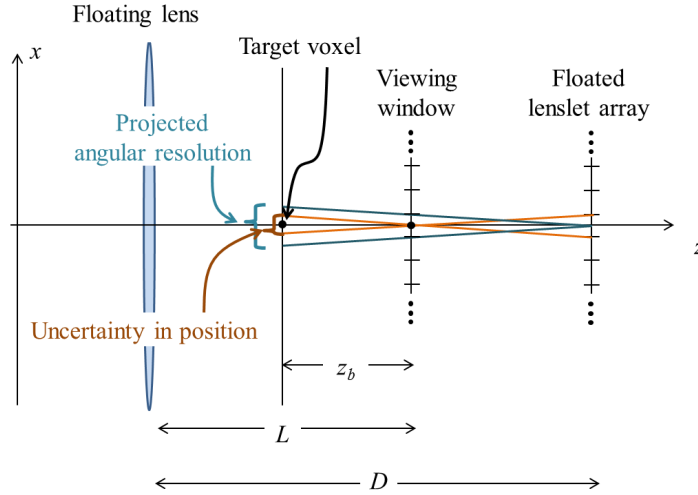


Fig. 2. Condition for avoiding discontinuity in motion parallax perceived by the human visual system. Discontinuity in motion parallax causes the uncertainty in the lateral position of the target voxel. This uncertainty should be smaller than the projected angular resolution of the viewing window to be compared in angular sense.

$$\Delta_v \frac{z_b}{|D-L|} < p_w \left(1 - \frac{z_b}{|D-L|} \right),$$

$$\Delta_v \frac{z_f}{|D-L|} < p_w \left(1 + \frac{z_f}{|D-L|} \right),$$
(6)

where z_b and z_f are the longitudinal displacement of the target voxel behind and in front of the viewing window, respectively. D is the distance between the floating lens and the floated lenslet array. In the aspect of visual quality, the condition given by Eq. (6) imposes a limitation on the expressible longitudinal range of 3D image. Using Eq. (6), the upper boundary for $z_f + z_b$, which can be regarded as a limitation in the expressible depth range, is calculated as

$$\Delta_z = z_f + z_b < \frac{2R_\theta p_w}{1 - (p_w/|D-L|)^2 R_\theta^2}.$$
(7)

Hence, the upper boundary given by Eq. (7), again, depends on the angular sampling rate R_θ .

As we investigated so far, the angular sampling rate on the viewing window of integral floating system affects visual quality of displayed 3D images. In the aspect of display, the expressible depth range is restricted, whereas, in the aspect of observer's perception, it is closely related to the discontinuities of motion parallax which are eventually related to the expressible depth range. In any aspects, increase in angular sampling rate improves related characteristics. However, without increase in the fundamental resource, other characteristics will be sacrificed to balance the tradeoff relationship. The lenslet array with $f = 22$ mm and $\varphi = 10$ mm and the floating lens with $F = 175$ mm have been usually adopted for the implementation of integral floating system [4–8]. We have chosen the integral floating system of these specifications, along with $g = 21.8$ mm, $G = 200$ mm and $p = 0.2$ mm, as a reference system. We have examined the changes in various features as the angular sampling rate of the reference system, R_θ , is increased to kR_θ , where k is a scaling factor. The scaling factor of angular sampling rate has been equally imposed to L and φ ; i.e., L has been scaled to $k^{1/2}L$ and

φ' has been scaled to $\varphi'/k^{1/2}$. p has been fixed to the original value, 0.2 mm. As shown in Fig. 3, the expressible longitudinal range of integral floating display is enhanced as the angular sampling rate is increased. However, we can see that it results in the sacrifice of other features because the fundamental resource has not been increased. Hence, we should find out the way to increase the angular sampling rate without sacrificing other features of integral floating system.

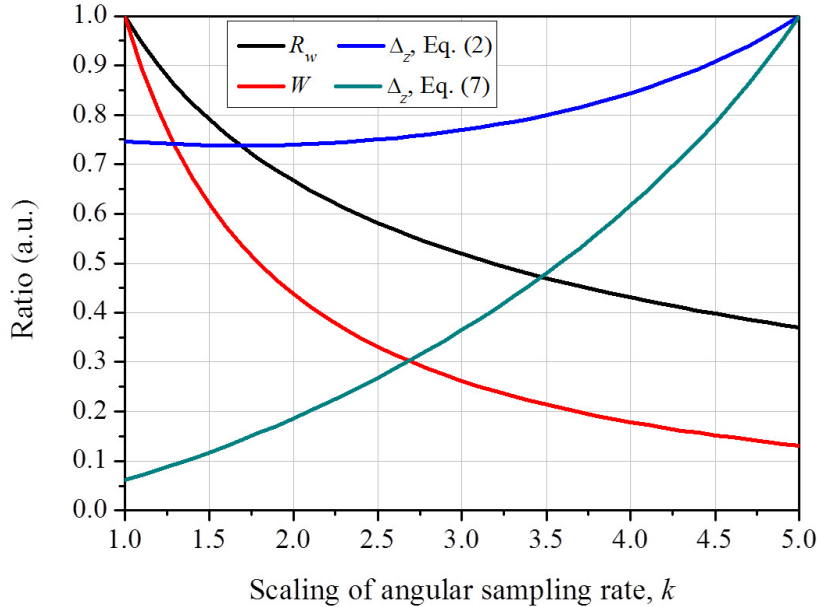


Fig. 3. Change in visual qualities of integral floating display according to the increase in angular sampling rate. k : scaling factor to the reference angular sampling rate; R_w : resolution of the viewing window; W : size of the viewing window; Δ_z : expressible longitudinal range calculated with Eqs. (2) or (7). R_w and W were normalized by the values at $k = 1$ while Δ_z by the value at $k = 5$.

3. Proposed methods

In this section, we propose two methods to increase the angular sampling rate on the viewing window of integral floating system based on the time-multiplexing principle by using the dynamically variable apertures. With our proposed methods, it is possible to increase the angular sampling rate without changing any other specifications. Hence, the characteristics bounded in the tradeoff relationship need not be sacrificed in return for enhanced angular sampling rate.

Figure 4 shows the brief diagram that describes the system configuration of our proposed method I. We will discuss the method only in x - z plane without loss of generality. Our purpose is to subdivide each angular sampling step on viewing window. Tracing rays back to the lenslet array plane, subdivided rays pass through different lateral positions on each lenslet as shown in Fig. 4. Hence, if we can separately address each subdivision of the angular sampling step, it will be possible to increase angular sampling rate on the viewing window. In our proposed method I, the lateral separation of lenslet aperture of the lenslet array is achieved by adopting the dynamically variable apertures (or slits for one-dimensional case) in front of the lenslet array. For n subdivisions of angular sampling step, the adopted aperture is composed of n slits per each lenslet, which can alternate its state between opened and blocked. Each subdivision of the angular sampling step can contribute to displaying 3D image only when the corresponding slit is open. The array of slits needs to change its shape through n phases to utilize time-multiplexing. In each phase, only one slit per each lenslet is open. The

slits are sequentially opened as the phase is changed. As we change an open slit per each lenslet, the addressed subdivision of angular sampling step also changes. After one period ends, whole subdivisions of angular sampling step can be addressed with different image information.

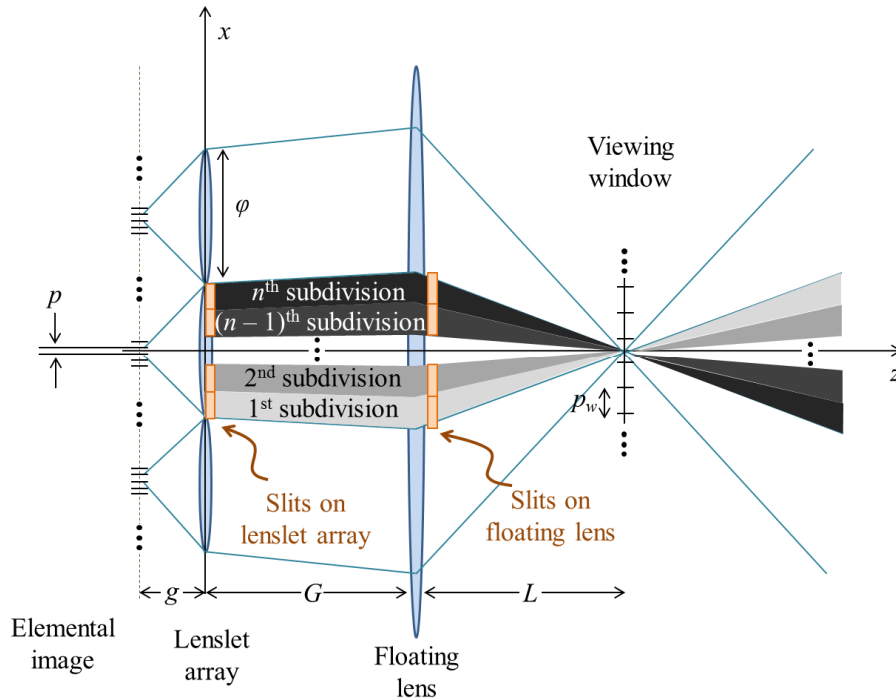


Fig. 4. Diagram describing the basic idea of proposed methods.

Figure 5 describes the relationship between the elemental image and the dynamically variable apertures, according to the phase, using the case of 3 subdivisions. As described above, for the conventional integral floating system, the elemental image region for each lenslet of the lenslet array can be generated by recording the image on the viewing window through the corresponding virtual pinhole. And each virtual pinhole coincides with the floated image of the center of corresponding lenslet on the lenslet array where the chief rays pass through. By introducing dynamically variable apertures (or slits) on the lenslet array, the rays passing through the center of open slit are considered as chief rays. Hence, $(n - 1)$ virtual pinholes are additionally created between each interval of conventional virtual pinholes. With these pinholes, the additional perspectives of the 3D image can be recorded and provided. For the generation of the elemental images, the location of each virtual pinhole, which is the floated position of the center of each aperture of the dynamically variable apertures, is calculated. As shown in Fig. 5, n virtual pinholes per each interval are sequentially opened as the phase changes. For each phase, the elemental image is generated and displayed using corresponding virtual pinholes. When n generated elemental images are displayed synchronized with the operation of the dynamically variable apertures, the angular sampling step can be subdivided by n .

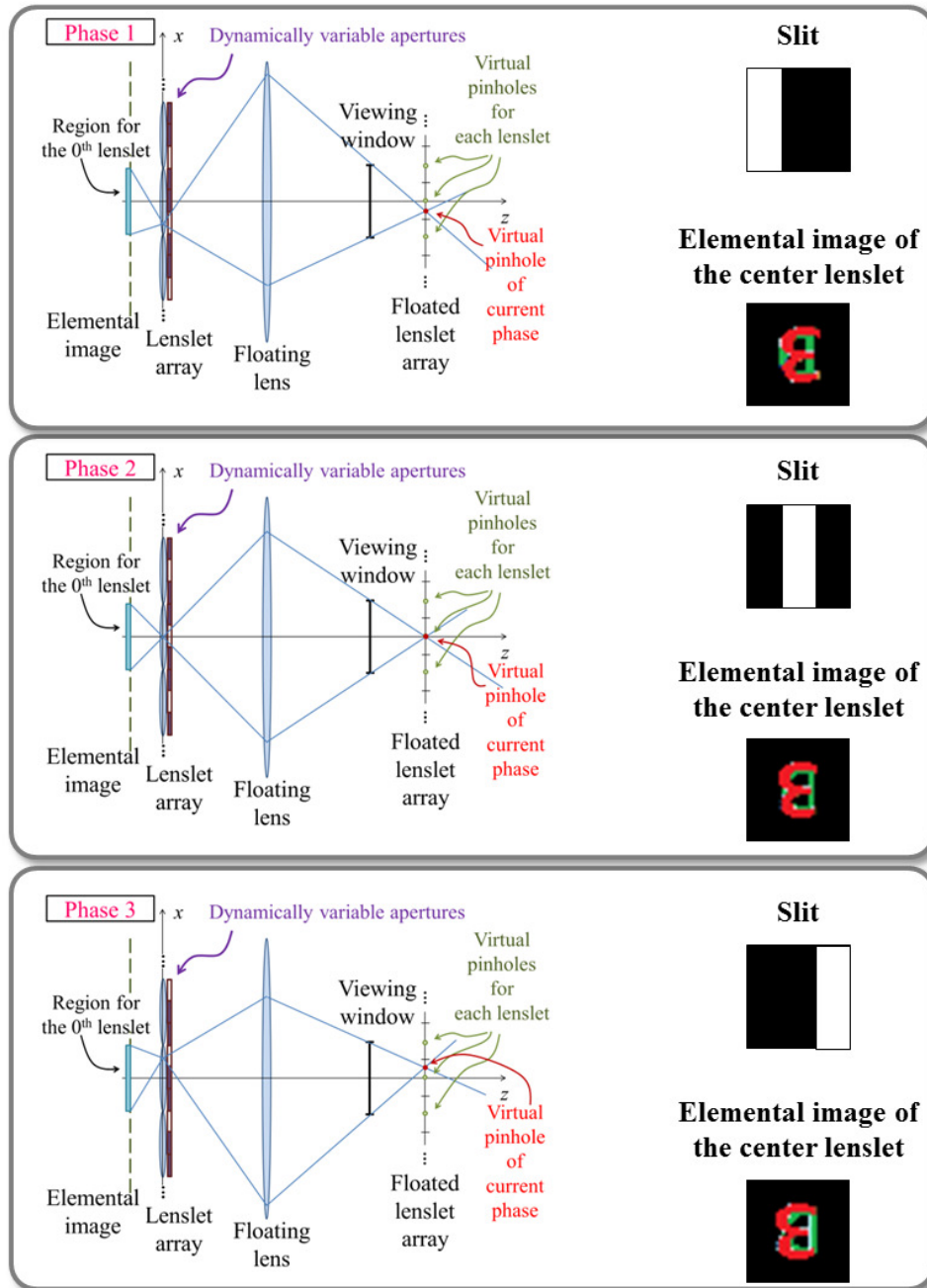


Fig. 5. Relationship between the elemental image and dynamically variable aperture for the case of 3 subdivisions in method I. The state of aperture and its corresponding elemental image of the center lenslet are provided as a reference for each phase. 3D objects are two characters '3' and 'D' located at different depths.

As shown in Fig. 4, the subdivision of the angular sampling step can also be achieved by locating the dynamically variable apertures in front of the floating lens instead of the lenslet array. In our method II, the angular sampling step of the integral floating display is subdivided by the dynamically variable apertures located in front of the floating lens. As the method I, one angular sampling step can be divided by n subdivisions with the aid of n slits. One

angular sampling step illuminates the lateral range of φ' on the floating lens and it should be covered by n slits of the dynamically variable apertures. Hence, the lateral size of each slit should be φ'/n . As with the method I, the n slits are opened sequentially and synchronized elemental images are displayed. The entire configuration and operation of method II is very similar with the method I. However, for the proposed method II, the way generating elemental image is totally different from the method I.

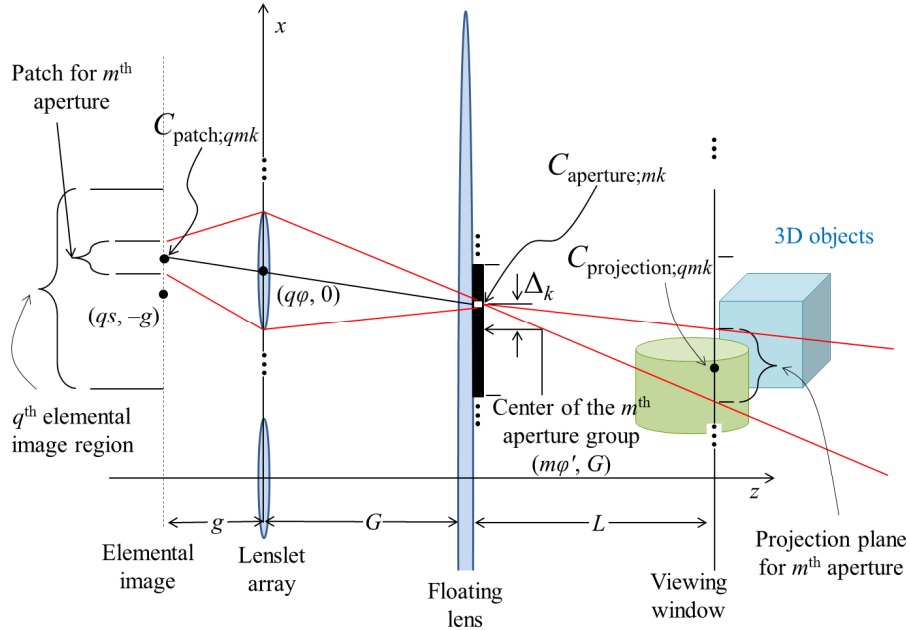


Fig. 6. Optical path of rays starting from one lenslet to viewing window via one aperture in the configuration of proposed method II.

Figure 6 shows the optical path of rays, whose envelope is indicated as red lines, passing through one lenslet and one aperture of method II. The center of lenslet array, floating lens and aperture array are assumed to be located at the origin in the lateral direction. As an example, the relationship between the q^{th} lenslet, whose center is at $(q\varphi, 0)$, and the m^{th} aperture group, whose center is at $(m\varphi', G)$, is illustrated. One aperture group is composed of n apertures for the case of n subdivisions, and it covers one angular sampling step on the floating lens. For the k^{th} aperture of the m^{th} aperture group, the coordinate of the center of aperture is $C_{\text{aperture};mk}(m\varphi' + \Delta_k, G)$, where Δ_k is the offset of the k^{th} aperture from the center of corresponding aperture group. For the q^{th} elemental image region, whose center is at $(qs, -g)$ where $s = \varphi g/f$, rays from only small patch of that region can pass through $C_{\text{aperture};mk}$. The center coordinate and length of this patch can be easily calculated as $C_{\text{patch};qmk}(qs + (q-m)\varphi'g/G - g\Delta_k/G, -g)$ and $\varphi'g/G$, respectively. On the right-hand side of the floating lens, this patch is floated as a part of the viewing window. We can set a relationship of the pinhole camera, considering that part of the viewing window as a projection plane, where the image is captured, and the aperture as a virtual pinhole. Regarding that the magnification between the elemental image and viewing window is $f(L - F)/F(g - f)$, the image of 3D objects is captured on the projection plane by the virtual pinhole camera with parameters:

$$\begin{aligned}
\text{Virtual pinhole:} & \quad (m\phi' + \Delta_k, G), \\
\text{Center of projection plane:} & \quad \left(\frac{f(L-F)}{F(g-f)} \left[\Delta_n \frac{g}{G} - (q-m)\phi' \frac{g}{G} \right], L+G \right), \quad (8) \\
\text{Size of projection plane:} & \quad \phi' \frac{g}{G} \frac{f(L-F)}{F(g-f)}.
\end{aligned}$$

The captured image is used for filling the corresponding patch of the q^{th} elemental image region. Repeating capturing process changing the value of m , the entire viewing window can be covered by captured images, and consequently the q^{th} elemental image region is generated. In the same way, other elemental image regions of the k^{th} phase can also be generated. Generating the elemental images for all the phases, n elemental images can be prepared that would be displayed synchronized with the operation of the dynamically variable apertures.

4. Experimental results

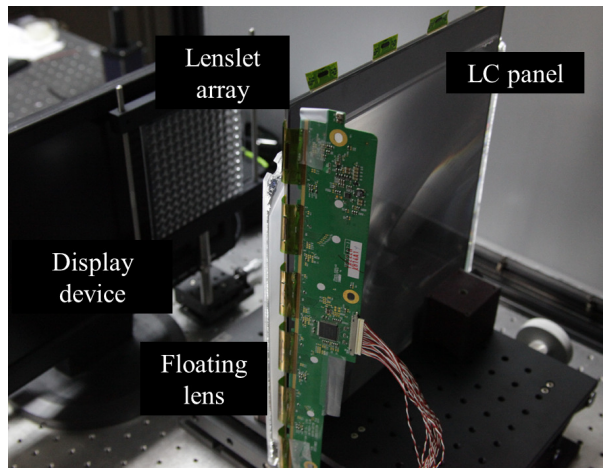


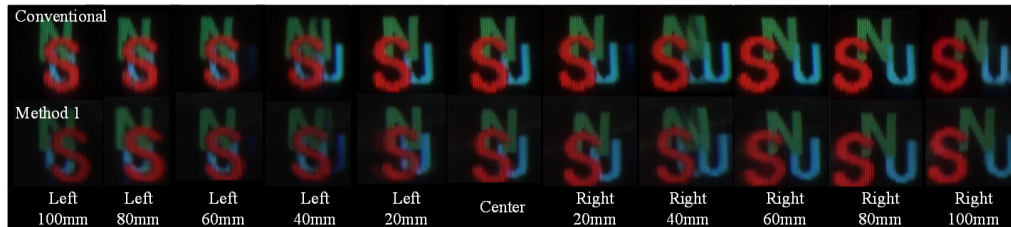
Fig. 7. System configuration of the prototype system implemented for the preliminary experiments.

To verify the feasibility of our proposed methods, we have implemented prototype systems and performed preliminary experiments with implemented systems. Figure 7 shows the experimental setup of our prototype system, which is configured for the method II. For the electronically controllable operation of dynamically variable apertures, we have adopted a commercially available liquid crystal (LC) panel for the implementation of apertures. The display device used for the experiments is also an LC panel and the displayed image has a certain polarization. For convenience, we have removed the polarizers attached to LC panel to be used for the apertures. In the implementation of the setup, the additional polarizer has been attached in front of LC panel, which is prepared for apertures, considering the polarization direction of display device. The experimental setup shown in Fig. 7 can be easily rearranged for the method I by simply moving the LC panel for aperture to the location in front of the lenslet array. Table 1 shows the detailed specifications of the implemented systems.

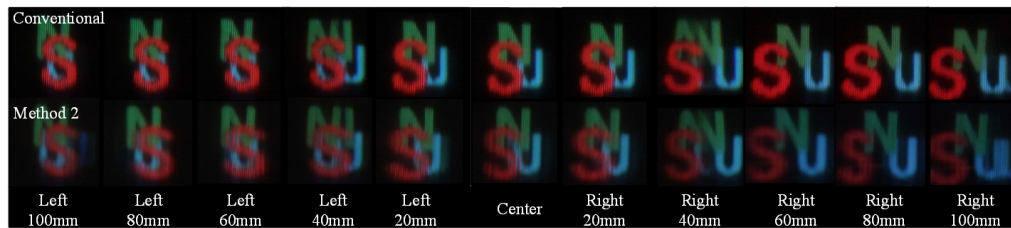
We have set $g = f$ and $G = 200$ mm. Along with specifications given in Table 1, these are parameters similar to those that usually appear [4–8]. To provide a complete image by time-multiplexing, the refresh rate of the apertures should be fast enough to avoid flickering perceived by human visual system. However, the LC panel adopted for the experiment has a refresh rate of 60 Hz. Though the higher frame rate is commercially available, it is enough for the purpose to prove the feasibility of our proposed methods. Hence, the experimental results of the proposed methods are images captured with sufficiently long exposure time.

Table 1. Specification of the Prototype

Lenslet array	f	Lenslet pitch	10 mm × 10 mm
		Focal length,	22 mm
		Total size	130 mm × 130 mm
Floating lens	F	Size	300 mm × 300 mm
		Focal length,	175 mm
LC panel (For aperture)		Pixel pitch	0.267 mm × 0.267 mm
		Resolution	1024 × 768
		Frame rate	60 Hz
LC panel (For display)		Pixel pitch	0.172 mm × 0.172 mm
		Resolution	1920 × 1200
		Frame rate	60 Hz



(a)



(b)

Fig. 8. Experimental results of displaying 3D image by the conventional integral floating display technique and the proposed methods I and II. The images have been captured moving around the center of the system. The distance between camera and the system was 1600 mm. (a) The comparison of motion parallax between the conventional method and the proposed method I, and (b) the comparison between the conventional method and the proposed method II.

Figure 8 shows the experimental results of displaying 3D image with the conventional and proposed integral floating systems. Target 3D image is composed of 3 characters ‘S’, ‘N’ and ‘U’, which are located at different longitudinal positions. ‘S’ and ‘U’ are located 150 mm in front and behind of the viewing window whereas ‘N’ is at the viewing window position. Figure 8 shows that the implemented systems express well the intended longitudinal positions of characters. Comparing leftmost images with rightmost ones, ‘S’ and ‘U’ sweep nearly full width of ‘N’, which is 20 mm, as the camera moves. This makes sense because the lateral displacement of ‘S’ and ‘U’ about ‘N’ is calculated to be approximately 21 mm when the observer, who is at 1600 mm distant from the floating lens, laterally moves 200 mm. For the proposed methods, 10 subdivisions have been made for one angular sampling step only in horizontal direction. Using Δ , in Eq. (3) and D in Fig. 2, the viewing angle of the center viewing zone can be calculated as approximately 3° . Hence the proposed methods subdivide the center viewing angle into about 0.3° for each subdivision. In Fig. 8, the 3D image displayed by conventional method shows 3 different perspectives. However, for the interval where the 3D image by the conventional scheme is stationary, motion parallax is investigated from the 3D images displayed by the proposed methods referring to Fig. 8. Hence, the results show that the angular sampling rate has been successfully increased by adopting the proposed

method I or II. When the observer is near the transition region, where the perspective changes for the conventional scheme, the distortion of the displayed 3D image is investigated for the conventional and proposed methods. In Fig. 8, results at left 40 mm or right 40 mm show artifact because they were captured at the transition region. This artifact will be discussed in the next section.

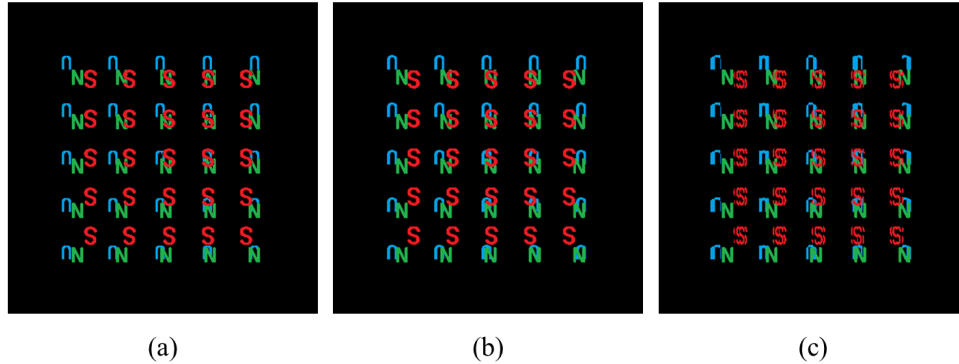


Fig. 9. Elemental images used for experiments. (a) Conventional scheme. (b) Phase 1 of proposed method I (Media 1). (c) Phase 1 of proposed method II (Media 2). Other phases of the proposed methods can be found in the movie files.

Figure 9 shows the elemental images used for displaying 3D images presented in Fig. 8. Because we have used 5×5 elemental image for the conventional scheme, the integral floating system can show 5×5 perspectives of displayed 3D image. For the proposed methods, the angular sampling rate has been increased 10 times larger in the horizontal direction. Hence, 10 elemental images should be time-multiplexed for each proposed method and they are provided as movie files in Fig. 9. Note that the elemental images for the proposed methods I and II are different.



Fig. 10. Displayed 2D image with the system configuration of proposed method II.

By implementing dynamically variable aperture with LC panel, the proposed method II can take one more advantage other than the enhancement of angular sampling rate. When the display device prepared for the elemental image displays a white image, it becomes merely a backlight unit for the LC panel in front of the floating lens. Hence, the entire system operates as 2D display by displaying 2D image on the LC panel in front of the floating lens. Using this configuration, 2D/3D convertible feature, which is one of important issues of 3D display, can be implemented for the integral floating system for the first time. Figure 10 shows an example of 2D image displayed following this scheme. The grid lines of lenslet array are slightly visible in the displayed 2D image.

5. Discussion

In Fig. 8, the distortion of the 3D image has been investigated near the transition region of the conventional method. When the observer is near the transition region, the 3D image is reconstructed by rays passing through near the edge of each lenslet of the lenslet array. Because the imaging principle of integral floating system is based on the thin lens approximation, these near-edge rays cause distortion in the 3D image displayed by integral floating scheme. The same explanation can be given to the distortion of proposed methods. Hence, though the angular sampling rate is increased by the proposed methods, the distortion of 3D image near the transition region cannot be resolved because it comes from the physical limitation of the lenslet array.

For the method II, there is one more reason that leads to the artifact of displayed 3D image. As an example, the optical paths of rays from the q^{th} lenslet are illustrated. Because of the finite pixel pitch of the display panel, the image on the viewing window is sampled discretely with a finite pitch, which was indicated as p_w in the previous sections. As described in Fig. 11, in the generation of the elemental image, the adjacent virtual pinhole cameras, which are determined by Eq. (8), usually share the same pixel at the edges of their projection planes. Hence, the crosstalk occurs at the edge of the projection plane of each virtual pinhole camera because of finite sampling pitch. In the viewpoint of display, images which are prepared for totally different directions conflict at the shared pixel. In the example of Fig. 11, the viewing direction #1 and #2 are overlapped at the shared pixel. This artifact cannot be resolved because it is based on the finite pixel pitch of display device. This kind of crosstalk appears when the observer is near the location of transition region in the conventional method.

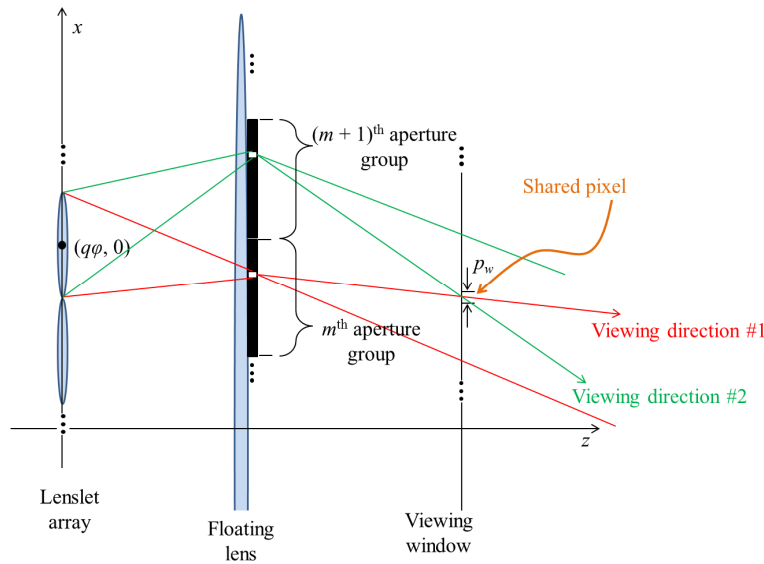


Fig. 11. Describing the reason for the crosstalk occurred in the proposed method II.

6. Conclusion

In this paper, we have proposed methods to enhance the angular sampling rate of the integral floating system by adopting dynamically variable apertures in front of the lenslet array or the floating lens. To enhance the angular sampling rate, one angular sampling step should be divided into a number of subdivisions. At one phase, the dynamically variable apertures allow only one subdivision per each angular sampling step to pass through. And the allowed subdivision is sequentially changed as the phase changes. Synchronizing with the properly generated elemental images, the dynamically variable aperture can enhance the angular

sampling rate by the time-multiplexing method. Instead of increasing the resolution of the display device, we have proposed the way to enhance angular sampling rate by using another resource, the frame rate.

The proposed methods will be helpful in improving visual quality of the integral floating display, especially for the expressible longitudinal range of 3D image. Moreover, for the configuration where the dynamically variable aperture is located in front of the floating lens, 2D/3D convertible feature can also be realized. To our knowledge, this is the first proposal that provides 2D/3D convertible feature to the integral floating display system.

Our proposed methods have been verified experimentally with the prototype system adopting LC panel for the implementation of dynamically variable apertures. However, the experimental results show that the artifact exists in 3D image when the observer is located near the region where the rays from the near-edge of each lenslet are used for display. The artifact is related to the fundamental limitation of integral floating scheme, such as the lens distortion or the finite pixel pitch of display device. Hence, further study will be needed to resolve such artifact of 3D image displayed by integral floating system.

Acknowledgment

This work was supported by the Brain Korea 21 Program (Information Technology, Seoul National University).